Biochimica et Biophysica Acta 1848 (2015) 2829–2838

Contents lists available at ScienceDirect

Biochimica et Biophysica Acta

journal homepage: www.elsevier.com/locate/bbamem

An *in vitro* study on the antioxidant capacity of usnic acid on human erythrocytes and molecular models of its membrane

M. Suwalsky [a,*], M. Jemiola-Rzeminska [b,c], C. Astudillo [a], M.J. Gallardo [d], J.P. Staforelli [d], F. Villena [e], K. Strzalka [b,c]

[a] Faculty of Chemical Sciences, University of Concepción, Concepción, Chile
[b] Faculty of Biochemistry, Biophysics and Biotechnology, Jagiellonian University, Krakow, Poland
[c] Malopolska Centre of Biotechnology, Jagiellonian University, Krakow, Poland
[d] Center for Optics and Photonics, University of Concepción, Concepción, Chile
[e] Faculty of Biological Sciences, University of Concepción, Concepción, Chile

ARTICLE INFO

Article history:
Received 3 June 2015
Received in revised form 17 August 2015
Accepted 19 August 2015
Available online 20 August 2015

Keywords:
Usnic acid
Erythrocyte membrane
Phospholipid bilayer
Antioxidant

ABSTRACT

Usnic acid (UA) has been associated with chronic diseases through its antioxidant action. Its main target is the cell membrane; however, its effect on that of human erythrocytes has been scarcely investigated. To gain insight into the molecular mechanisms of the interaction between UA and cell membranes human erythrocytes and molecular models of its membrane have been utilized. Dimyristoylphosphatidylcholine (DMPC) and dimyristoylphosphatidylethanolamine (DMPE) were chosen as representative of phospholipid classes located in the outer and inner monolayers of the erythrocyte membrane, respectively. Results by X-ray diffraction showed that UA produced structural perturbations on DMPC and DMPE bilayers. DSC studies have indicated that thermotropic behavior of DMPE was most strongly distorted by UA than DMPC, whereas the latter is mainly affected on the pretransition. Scanning electron (SEM) and defocusing microscopy (DM) showed that UA induced alterations to erythrocytes from the normal discoid shape to echinocytes. These results imply that UA molecules were located in the outer monolayer of the erythrocyte membrane. Results of its antioxidant properties showed that UA neutralized the oxidative capacity of HClO on DMPC and DMPE bilayers; SEM, DM and hemolysis assays demonstrated the protective effect of UA against the deleterious oxidant effects of HClO upon human erythrocytes.

1. Introduction

Usnic acid (UA) [(R)-1,1′-(1,7,9-trihydroxy-8,9b-dimethyl-3-oxo-3,9b-dihydrodibenzo[b,d]furan-2,6-diyl)diethanone; $C_{18}H_{16}O_7$, Fig. 1] is a yellow cortical pigment produced by a series of lichen species. It is a product of the secondary metabolism of the fungal partner and it exists in two enantiomers which differ in the orientation of the angular methyl group located in position 9b (Fig. 1) [1]. Several biological properties have been observed from this compound, such as gastroprotective, cardiovascular, cytoprotective, immunostimulatory, antimicrobial, anti-inflammatory and anticarcinogenic activities [1–5]. Chronic diseases are characterized by an enhanced state of oxidative stress, which results from an imbalance between the production of reactive species and antioxidant defense activity. UA has been associated with many chronic diseases mostly due to its antioxidant action in reducing oxidative damage. A review of the antioxidant potential of UA reported that it promoted the increase of superoxide dismutase (SOD), glutathione peroxidase (GPx), total glutathione (GSH) and constitutive nitric oxide synthase (cNOS) activities through the reduction of catalase (CAT), glutathione reductase (GR), lipid peroxidation (LPO), inducible nitric oxide synthase (iNOS) and myeloperoxidase (MPx) activities [2].

In the attempt to elucidate the molecular mechanisms of the interaction of UA with cell membranes, human erythrocytes and molecular models of its membrane were used. Human erythrocytes were chosen because of their only one membrane and no internal organelles, which constitute an ideal cell system for studying interactions of chemical compounds with cell membranes [6]. On the other hand, although less specialized than many other cell membranes they carry on enough functions in common with them such as active and passive transport, and the production of ionic and electric gradients to be considered representative of the plasma membrane in general. The molecular models of the erythrocyte membrane consisted in bilayers of dimyristoylphosphatidylcholine (DMPC) and dimyristoylphosphatidylethanolamine (DMPE), representative of phospholipid classes located in the outer and inner monolayers of cell membranes, particularly of the human erythrocyte, respectively [7,8]. The capacity of UA to perturb the bilayer structures of DMPC and DMPE was evaluated by X-ray diffraction and differential scanning

Abbreviations: UA, usnic acid; DMPC, dimyristoylphosphatidylcholine; DMPE, dimyristoylphosphatidylcholine; SEM, scanning electron microscopy; DM, defocusing microscopy.

* Corresponding author.
E-mail address: msuwalsk@udec.cl (M. Suwalsky).

http://dx.doi.org/10.1016/j.bbamem.2015.08.017
0005-2736/

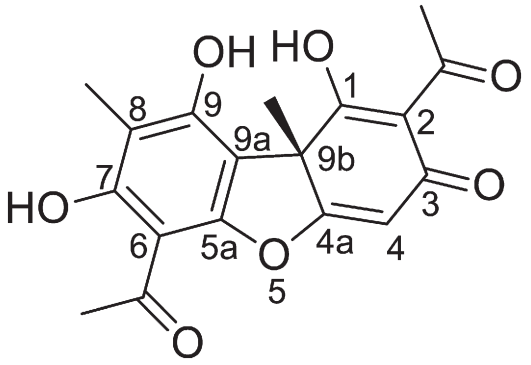

Fig. 1. Structural formula of (R) usnic acid (UA).

calorimetry (DSC); intact human erythrocytes were observed by scanning electron (SEM) and defocusing microscopy (DM). These systems and techniques have been used in our laboratories to determine the interaction with and the membrane-perturbing effects of other chemical compounds, particularly of native plant extracts [9–12]. The antioxidant properties of UA were evaluated in the molecular models of the erythrocyte membrane and human erythrocytes *in vitro* exposed to the oxidative stress induced by hypochlorous acid (HClO). HClO is a powerful natural oxidant that damages bacteria, endothelial cells, tumor cells and erythrocytes [13–16].

2. Materials and methods

2.1. Chemicals

Synthetic DMPC (lot 140PC-246, MW 677.9), DMPE (lot 140PE-60, MW 635.9) from Sigma (AL. USA) and usnic acid (R-enantiomer, lot MKBP1746V, MW 344.32 from Sigma-Aldrich, AL, USA) were used without further purification. Composition of phosphate buffered saline (PBS) was 150 mM NaCl, 1.9 mM NaH_2PO_4, 8.1 mM Na_2HPO_4, pH 7.4. Concentration of HClO from commercial samples was spectrophotometrically determined at 292 nm ($\varepsilon = 350\ M^{-1}\ cm^{-1}$) [17].

2.2. X-ray diffraction studies of DMPC and DMPE multilayers

The capacity of UA to perturb the structures of DMPC and DMPE multilayers was evaluated by X-ray diffraction. About 2 mg of each phospholipid was introduced into Eppendorf tubes which were then filled with 180 L of (a) distilled water (control), and (b) UA aqueous solutions in a range of concentrations (0.5–5.0 mM). The specimens were shaken, incubated for 15 min at 30 °C and 60 °C with DMPC and DMPE, respectively and centrifuged for 20 min at 2500 rpm. Samples were then transferred to 1.5 mm diameter special glass capillaries (Glas-Technik & Konstruktion, Berlin, Germany) and X-ray diffracted utilizing Ni-filtered CuKα radiation from a Bruker Kristalloflex 760 (Karlsruhe, Germany) X-ray system. Specimen-to-film distances were 8 and 14 cm, standardized by sprinkling calcite powder on the capillary surface. The relative reflection intensities were obtained in an MBraun PSD-50M linear position-sensitive detector system (Garching, Germany); no correction factors were applied. The experiments were performed at 18 °C ± 1 °C, which is below the main phase transition temperature of both DMPC and DMPE. Higher temperatures would have induced transitions onto fluid phases making the detection of structural changes harder. Each experiment was performed in triplicate.

2.3. Differential scanning calorimetry (DSC) studies on DMPC and DMPE liposomes

Appropriate amounts of chloroform solutions of DMPC or DMPE and UA were gently evaporated to dryness under a stream of gaseous nitrogen until a thin film on the wall of the glass test tube was formed. To remove the remnants of moisture, the samples were subsequently exposed to vacuum for 1 h and then dry lipid films were suspended in distilled water. The multilamellar liposomes (MLVs) were prepared by vortexing the samples at the temperature above gel-to-liquid crystalline phase transition of the pure lipid (about 30 °C for DMPC and 60 °C for DMPE). DSC experiments were performed using a NANO DSC Series III System with Platinum Capillary Cell (TA Instruments). The calorimeter was equipped with the original data acquisition and analysis software. In order to avoid bubble formation during heating mode the samples were degassed prior to being loaded by pulling a vacuum of 0.3–0.5 atm. on the solution for a period of 10–15 min. Then the sample cell was filled with about 400 μL of MLV suspension and an equal volume of buffer was used as a reference. The cells were sealed and thermally equilibrated for about 10 min below starting temperature of the run. All measurements were made on samples under 3-bar pressure. The data were collected in the range of 0–40 °C (DMPC) and 30–70 °C (DMPE) at the scan rate 1 °C min^{-1} both for heating and cooling. Scans of buffer as a sample and a reference were also performed to collect the apparatus baseline. For the check of the reproducibility each sample was prepared and recorded at least three times. Each data set was analyzed for thermodynamic parameters with the software package supplied by TA Instruments.

2.4. Scanning electron microscopy (SEM) studies on human erythrocytes

In order to perform the assays, three to four blood drops from a human healthy donor not receiving any pharmacological treatment were obtained by puncture of a finger and received in an Eppendorf tube containing 10 μL of heparin (5000 UI/mL) in 990 μL of phosphate buffer saline (PBS), pH 7.4. Red blood cell (RBC) suspension was then centrifuged (1000 rpm × 10 min), washed three times in PBS, the supernatant was discarded and replaced by the same volume of PBS. 150 μL was distributed in several Eppendorf tubes, centrifuged, the supernatant was disregarded, and usnic acid in PBS in a range of concentrations (2.5 μM–10 mM) was added to each tube and then incubated at 37 °C for 1 h, period in line with the larger effects induced by compounds on red cell shape [18,19]. Controls were cells resuspended in PBS without UA. After the incubation, samples were centrifuged (1000 rpm × 10 min), the supernatant disregarded, washed three times with PBS, and specimens were then fixed overnight at 4 °C by adding one drop of each sample to plastic tubes containing 500 μL of 2.5% glutaraldehyde in distilled water, reaching a final fixation concentration of about 2.4%. Samples were washed trice in distilled water and centrifuged (1000 rpm × 10 min.); about 40 μL of each sample were placed on siliconized Al glass covered stubs, air-dried at room temperature, gold coated for 3 min at 13.3 Pa in a sputter device (Edwards S 150, Sussex, England) and examined in a scanning electron microscope (JEOL JSM-6380LV, Japan). Data were expressed as mean ± standard deviation of 50 cell counts.

2.5. Optical and defocusing microscopy (DM) studies of human erythrocytes

Erythrocyte shapes were visualized and then analyzed through three dimensional reconstructions using defocusing microscopy (DM). The experiments were carried out at room temperature (about 18 °C) in an inverted optical microscope Nikon Eclipse Ti–U (Nikon, Tokyo, Japan), where the light source is provided by a halogen lamp with a transmission filter centered at 650 nm to avoid physical damage on red blood cells (RBCs). The objective was mounted on a C-focus system (Mad City Labs, Madison, USA) for a nanometric control of the focal plane position. The visualization was done with a High Resolution CMOS Camera, with Monochrome Sensor (Thorlabs, New Jersey, USA). RBCs were obtained from a healthy donor under no pharmacological treatment. RBC solution was prepared diluting the washed blood 20 times in a solution of PBS 1× and BSA 1 mg/mL. Usnic acid solution

was prepared in the same preparation of PBS and BSA. In order to carry out the analysis, RBC diluted solution was placed in a cuvette, and visualized at the optical microscope. After that, a morphologically normal erythrocyte was selected and the concentration of usnic acid was increased. In order to make three-dimensional reconstructions two images were captured in the defocus positions 0 and +2 μm at each concentration [20–22].

2.6. Hemolysis assays

Red blood cells (RBCs) were obtained from a healthy consenting donor. 10 mL of heparinized blood was centrifuged (EYDAM, Germany) at 2500 rpm for 10 min. After removal of plasma and buffy coat, the RBCs were washed three times with PBS at room temperature, and resuspended in PBS three times its volume for subsequent analyses [23]. RBCs (10% v/v) were incubated in a shaking bath for 15 min at 37 °C in PBS in the presence of increasing concentrations of UA in a final 1.5 mL volume. After cooling, increasing concentrations of HClO in PBS were added and centrifuged at 2500 rpm for 5 min. Hemolysis was spectrophotometrically evaluated (Jasco, Japan) at 540 nm as hemoglobin (Hb) released from cells in the supernatant [24]. Results were related to control (100% hemolysis induced by 2.5 mM HClO on RBC).

3. Results

3.1. X-ray diffraction studies of DMPC and DMPE multilayers

Fig. 2A exhibits results obtained by incubating DMPC with water and UA. As expected, water altered the structure of DMPC as its bilayer repeat (phospholipid bilayer width plus the layer of water) increased from about 55 Å in its dry crystalline form to 65 Å when immersed in water, and its small-angle reflections, which correspond to DMPC polar terminal groups, were reduced to only the first two orders of the bilayer width [25]. On the other hand, only one strong reflection of 4.2 Å showed up in the wide-angle region which corresponds to the average distance between fully extended acyl chains organized with rotational disorder in hexagonal packing. These results were indicative of the fluid state reached by DMPC bilayers. Fig. 2A discloses that after being exposed to increasing UA concentrations there was a gradual weakening of the small- and wide-angle lipid reflection intensities (indicated as SA and WA in the figure, respectively) which with 2 mM UA the 4.2 Å wide-angle reflection practically disappeared. From these results it can be concluded that UA produced a significant structural perturbation of DMPC bilayers in the 0.5–2 mM range of concentrations. However, increasing UA concentrations induced a reordering of DMPC bilayers indicated by the resulting increase of the reflections intensities, which with 5 mM UA showed the same X-ray pattern of control. Fig. 2B shows the results of the X-ray diffraction analysis of DMPE bilayers incubated with water and UA. As reported elsewhere, water did not significantly affect the bilayer structure of DMPE [25]. Fig. 2B shows that UA in the 0.5–5 mM range caused a significant and gradual weakening of DMPE reflection intensities.

Fig. 3 presents the protective capacity of UA on the oxidative property of HClO in DMPC and DMPE bilayers. Fig. 3A shows that from 3 mM to 5 mM HClO concentration there was an increasing perturbation of DMPC bilayer structure. However, as it can be appreciated in Fig. 3C, in the 2 to 4 mM concentration UA neutralized the deleterious effect of 5 mM HClO; however, 5 mM HClO in the presence of 5 mM UA induced a structural perturbation of DMPC bilayers. The same experiments performed in DMPE showed that while 5 mM HClO induced a deep perturbation to DMPE bilayer structure (Fig. 3B), this effect was completely neutralized by 3 mM UA (Fig. 3D).

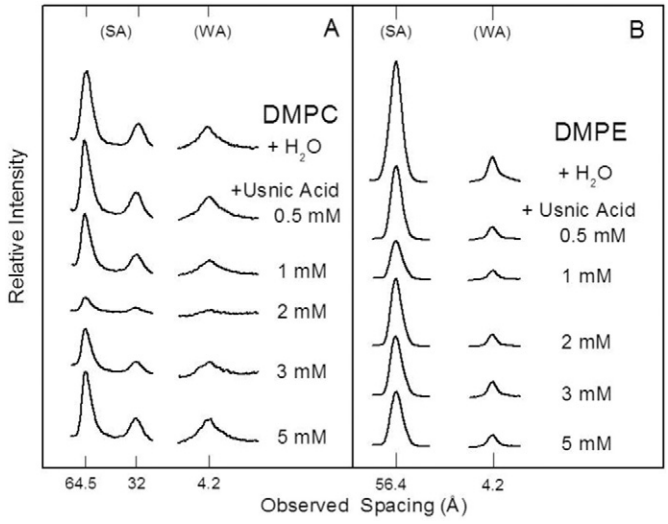

Fig. 2. X-ray diffraction patterns of (A) dimyristoylphosphatidylcholine (DMPC) and (B) dimyristoylphosphatidylethanolamine (DMPE) in water and usnic acid (UA); (SA) small-angle and (WA) wide-angle reflections.

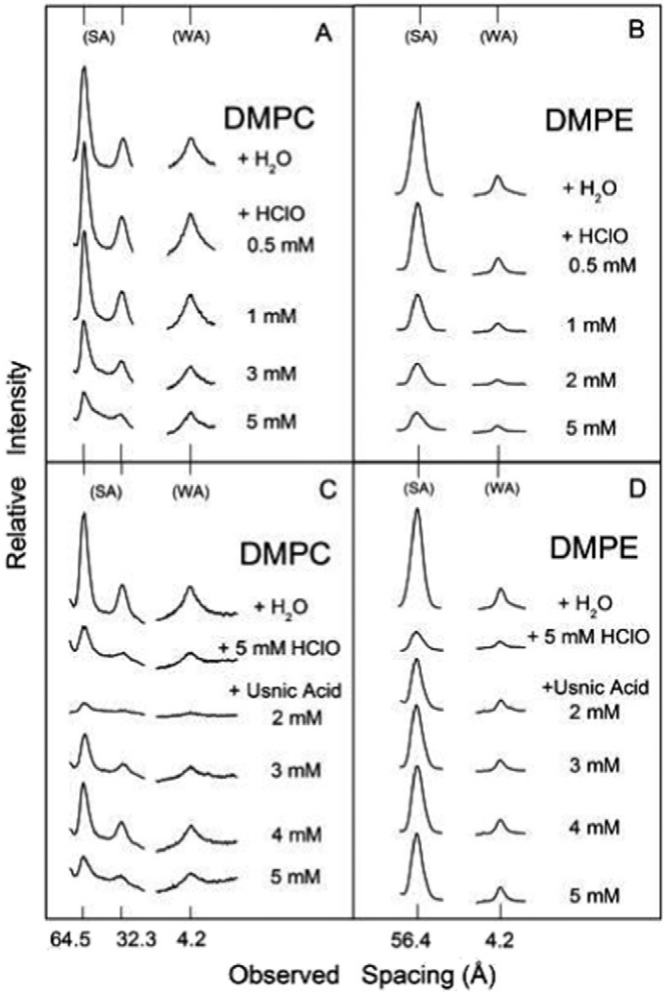

Fig. 3. X-ray diffraction patterns of (A) dimyristoylphosphatidylcholine (DMPC) in water and HClO; (B) dimyristoylphosphatidylcholine (DMPC) in water, usnic acid (UA) and HClO; (C) dimyristoylphosphatidylethanolamine (DMPE) in water, and HClO; (D) dimyristoylphosphatidylethanolamine (DMPE) in water, UA and HClO; (SA) small-angle and (WA) wide-angle reflections.

3.2. Differential scanning calorimetry (DSC) studies on DMPC and DMPE liposomes

The representative high-sensitivity DSC heating thermograms obtained for pure DMPC multibilayer vesicles and binary mixtures of DMPC and UA at 0.1 to 5 mM content are shown in Fig. 4A. In the thermal range of 0–30 °C, fully hydrated DMPC bilayers in the absence of any additives, underwent a strong and sharp main-transition at 23.83 °C, with an enthalpy change (ΔH) of 21.54 kJ mol^{-1}, which corresponded to the conversion of the rippled gel phase ($P_{\beta'}$) to the lamellar liquid-crystal $L_{\beta'}$ phase. At 14.71 °C with a ΔH of 2.86 kJ mol^{-1} occurred the smaller transition ($L_{\beta'} \rightarrow P_{\beta'}$ phase transition), so called pretransition. Here, the transition temperatures correspond to the transition peak at the maximal peak heat, and the transition enthalpies correspond to the integrated area under the peak divided by the lipid concentration. The results for the thermodynamic data of the pure DMPC are in agreement with previous reports (for reviews see references [26,27]). The set of parameters determined on the basis of heating and cooling scans obtained for DMPC/UA mixtures is given in Table 1. Considering DMPC profile changes upon incorporation of UA, one should give weight to the pretransition, which was lost for such a low amount as 0.5 mM during heating and not observed at 0.1 mM during cooling. This may suggest much stronger interactions between UA molecules (or their moiety) with polar headgroup region. Although the temperature of main phase transition was not significantly affected by the presence of UA and not concentration dependent (ΔT = ~0.7) for 0.5, 1, and 5 mM (see Fig. 4B), the peaks are gradually lowered and broadened. As a whole, it may imply that UA molecules were located in close vicinity of the lipid bilayer surface in such a way that they could distort melting of DMPC fatty acid chains only to some extent. Illustrated in Fig. 5 are representative high-sensitive DSC heating thermograms obtained for DMPE and DMPE liposomes containing UA. In the thermal range of 30–70 °C, the pure DMPE bilayers exhibited a strong and sharp main-transition at 50.64 °C, with an enthalpy change (ΔH) of 28.15 kJ mol^{-1}, arising from the conversion of gel to liquid-crystal phase. The transition was reversible and the shape of the peak is roughly symmetrical. Table 2 present values of thermodynamical parameters determined for DMPE/usnic acid mixtures, of which those for pure DMPE are concurrent with the literature data [28]. The calorimetric profiles obtained for DMPE were distorted by the presence of UA, especially in terms of peak height and width. The shift in temperature of phase transition towards lower values was observed; however, it was not really pronounced (less than 1 °C for heating and a bit more than 2 °C for cooling) even at such a high UA content as 1 mM (see Fig. 5B). Additionally, in the case of the sample with 2 mM UA it could be observed an appearance of the low temperature shoulder, which was undergoing a shift towards lower temperatures under successive heating scans as indicated in Fig. 6.

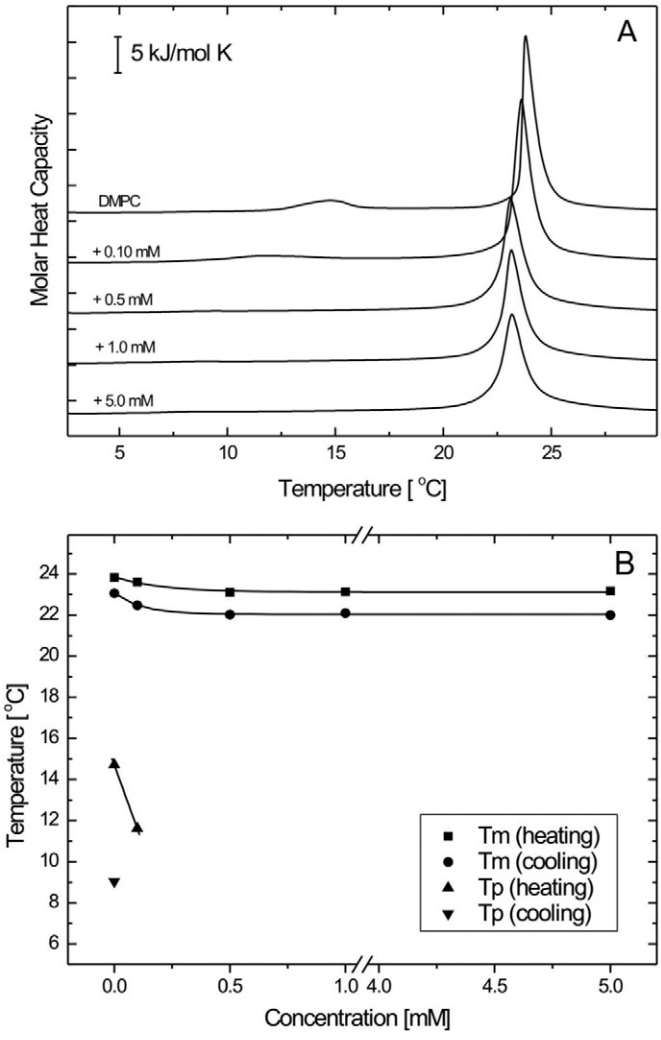

Fig. 4. (A) Representative DSC curves obtained for multilamellar DMPC liposomes containing usnic acid (UA) in the concentration range of 0 to 5 mM. Scans were obtained at a heating rate of 1 °C min^{-1}; (B) Plot of pretransition and main phase transition temperatures of DMPC multilamellar liposomes determined for heating and cooling scans as a function of UA content.

3.3. Scanning electron microscopy (SEM) studies of human erythrocytes

The effects of the interaction of UA with human erythrocytes were *in vitro* evaluated by SEM. The resulting micrographs (Fig. 7) show that the UA induced changes in the morphology of the red blood cells. The normal resting shape of the human red blood cell is a flat biconcave disc (discocyte) ~8 μm diameter which can be observed in Fig. 7A, corresponding to the erythrocytes incubated with PBS (pH 7.4) (control). On the other hand, morphological analysis of the results revealed that UA changed the normal shape of the red blood cells in a dose-dependent manner. Fig. 7B (10 μM) clearly shows that discocytes underwent a partial transformation into echinocytes (erythrocytes with crenated shapes), and knizocytes (cells with two or three concavities due to indentations in the cell membrane), and 1 mM UA (Fig. 7C) increased the number of echinocytes. Figs. 8 and 9 present the protective capacity of UA on the oxidative property of HClO in human erythrocytes. Fig. 8B shows that 0.5 mM HClO induced the formation of stomatocytes (cup-shaped cells), which considerably increased with 1.25 mM HClO (Fig. 8C). However, as it can be appreciated in Fig. 9, the shape alteration induced by HClO was reversed in samples previously incubated with UA. In fact, cells incubated with 2.5 μM UA and 1.25 mM HClO still show a large number of stomatocytes (Fig. 9C), but it can also be seen a few normal cells (shown by arrows), whose number increased when UA concentration was 7.5 μM (Fig. 9D). These results demonstrate the protective effect of UA in very low concentrations against the shape perturbing effect of HClO upon human erythrocytes.

3.4. Defocusing microscopy (DM) studies of human erythrocytes

Red blood cells were observed and analyzed with wide field optical microscopy. The effect of UA on red blood cells was visualized and analyzed using defocusing microscopy (DM) technique. The goal was to characterize the morphological changes of the cells when the concentration of UA was increased in the solution. Fig. 10 shows the effects of UA in RBC morphology at μM concentrations. This compound induced changes from the normal discoid erythrocyte shape into an echinocyte one, as observed in the 3D reconstruction (Fig. 10B). At low concentration of UA (2 μM) cells have the same morphology than the control cells, and at 100 μM all the erythrocytes were transformed into echinocytes

Table 1
Thermodynamic parameters of the pretransition and main phase transition of pure, fully hydrated DMPC multilamellar liposomes and DMPC/usnic acid mixtures determined from heating and cooling scans collected at a heating (cooling) rate of 1 °C min^{-1}. The accuracy for the main phase transition temperature and enthalpy was ±0.01 °C and ±0.8 kJ/mol, respectively.

Compound	Pretransition heating			Main transition heating			Pretransition cooling			Main transition cooling		
Conc [mM]	ΔH [kJ/mol]	ΔS [J/mol K]	T_m [°C]	ΔH [kJ/mol]	ΔS [J/mol K]	T_m [°C]	ΔH [kJ/mol K]	ΔS [J/mol K]	T_m [°C]	ΔH [kJ/mol]	ΔS [J/mol K]	T_m [°C]
DMPC												
1.0	2.86	0.99	14.71	21.54	7.25	23.83	1.30	0.46	9.04	20.34	6.87	23.06
+ usnic acid												
0.1	2.08	0.77	11.62	27.30	9.20	23.62	–	–	–	25.44	8.61	22.48
0.5	–	–	–	21.24	7.17	23.11	–	–	–	20.93	7.09	22.03
1.0	–	–	–	20.51	6.92	23.14	–	–	–	18.62	6.31	22.10
5.0	–	–	–	21.10	7.12	23.18	–	–	–	17.32	5.87	22.00

(Fig. 10A). To observe if UA had a morphological protective effect against HClO, a solution of RBC incubated previously with 2 μM UA was prepared. Then, the concentration of HClO was increased until stomatocytes were formed. Fig. 11 shows the protective effect of usnic acid against HClO (Fig. 11A). 3D reconstruction (Fig. 11B) demonstrated the protective effect of UA against the shape perturbing effect of HClO upon human erythrocytes at 79.5 μM. It is important to note that 2 μM UA did not induce morphological changes to the cell (Fig. 10B).

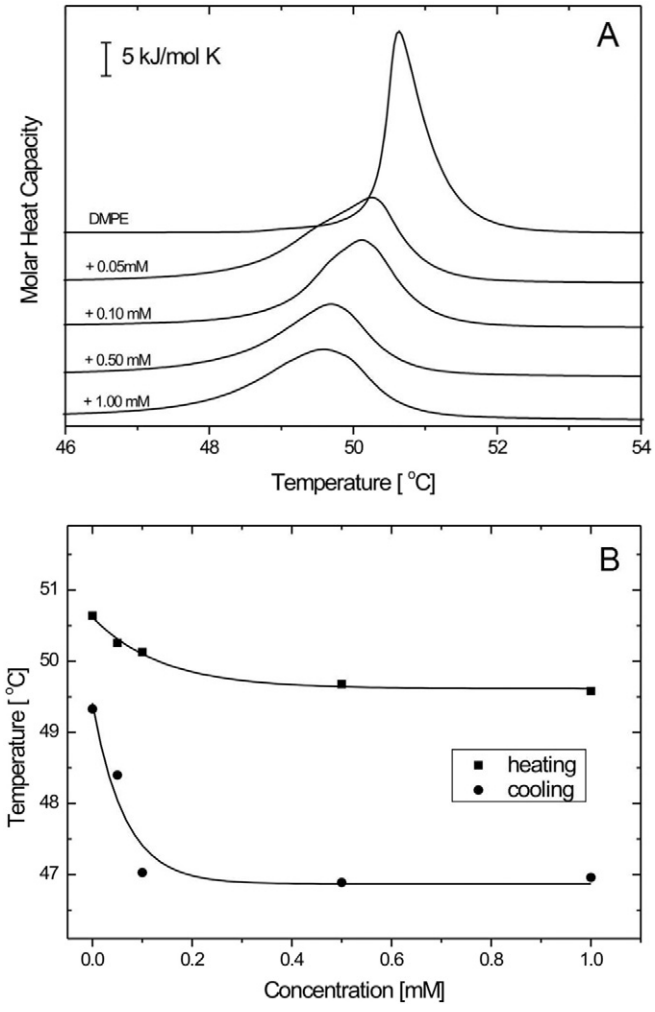

Fig. 5. (A) Representative DSC curves obtained for multilamellar DMPE liposomes containing usnic acid (UA) in the concentration range of 0 to 1 mM. Scans were obtained at a heating rate of 1 °C min^{-1}; (B) Plot of main phase transition temperature of DMPE multilamellar liposomes determined for heating and cooling scans as a function of UA content.

3.5. Hemolysis assays

Increasing concentrations of UA in the 5–17.5 μM range did not significantly increased the % of hemolysis (Fig. 12). However, the same range of concentrations gradually reduced the hemolytic effect of 1.25 mM HClO, which reached a value of 21% with 12.5 μM UA.

4. Discussion

With a broad spectrum of antimicrobial, anti-inflammatory and anticancer activities, usnic acid as a natural compound produced by several lichen species should be of great medical and biotechnological interest. However, despite its potential medical applications, its hepatotoxicity in mammals might prevent its use as a drug [29]. To overcome the toxicity of usnic acid, lipid-associated drug formulations that control drug delivery and release could be used. Among them, liposomes with their composition resembling the biological membranes may be considered as good candidates for an alternative biomaterial to be used for the encapsulation [30]. Therefore, studies on usnic acid–biomembrane interaction are prerequisite to understand its biological action.

In the present study, the interaction and antioxidant property of usnic acid (UA) were evaluated on human erythrocytes and molecular models of its membrane. The latter consisted in DMPC and DMPE bilayers, classes of lipids preferentially located in the outer and inner monolayers of the human erythrocyte membrane, respectively [7,8]. Herein, the thermodynamics of UA interaction with lipid model systems was investigated in terms of induced perturbation of the lipid phase transition using differential scanning calorimetry, whereas the structural changes accompanying interactions between lipids and usnic were monitored by X-ray diffraction. Results by X-ray diffraction on the interaction of UA with DMPC bilayers in the gel phase showed that 2 mM UA produced a significant structural perturbation of the lipid bilayer in both the acyl and polar head regions of DMPC; however, increasing UA concentrations reversed this effect. Similar effects were observed in DMPE as

Table 2
Thermodynamic parameters of the phase transition of pure, fully hydrated DMPE multilamellar liposomes and DMPE/usnic acid mixtures determined from heating and cooling scans collected at a heating (cooling) rate of 1 °C min^{-1}. The accuracy for the main phase transition temperature and enthalpy was ±0.01 °C and ±0.8 kJ/mol, respectively.

Compound	Heating			Cooling		
Conc [mM]	ΔH [kJ/mol]	ΔS [J/mol K]	T_m [°C]	ΔH [kJ/mol]	ΔS [J/mol K]	T_m [°C]
DMPE						
1.00	28.15	8.70	50.64	22.35	6.93	49.33
+ usnic acid						
0.05	20.26	6.26	50.26	21.12	6.57	48.40
0.10	17.66	5.46	50.13	18.56	5.80	47.03
0.50	17.56	5.44	49.68	17.42	5.44	46.89
1.00	19.53	6.05	49.58	19.39	6.06	46.96

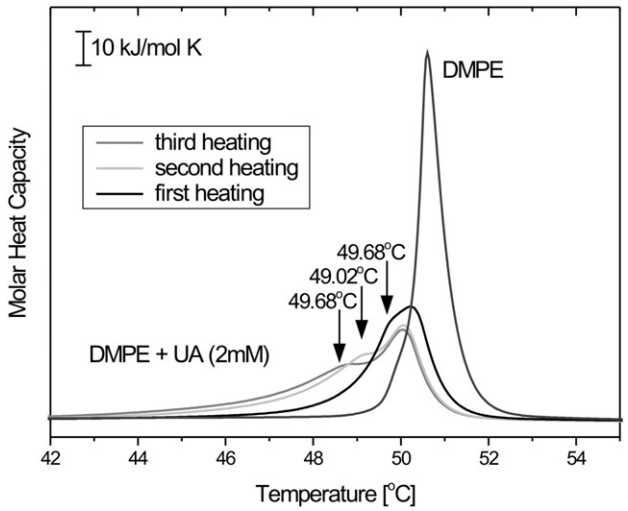

Fig. 6. Representative DSC curves obtained for multilamellar DMPE liposomes and those containing 2 mM usnic acid (UA) at successive heating scans. Scans were obtained at a heating rate of 1 °C min^{-1}.

1 mM UA induced a structural perturbation, which were also reversed with increasing UA concentrations. DMPC and DMPE differ only in their terminal amino groups, these being $^{+}N(CH_3)_3$ in DMPC and $^{+}NH_3$ in DMPE. Moreover, both molecular conformations are very similar in their dry crystalline phases with the hydrocarbon chains mostly parallel and extended and the polar groups lying perpendicularly to them [25]. However, DMPE molecules pack tighter than those of DMPC. This effect, due to DMPE smaller polar groups and higher effective charge, stands for a very stable multibilayer system which is not significantly affected by water [25]. Therefore, it is somewhat surprising that despite the strong hydrogen bond network and electrostatic interactions of DMPE bilayers UA was able to interact and perturb its structure. On the other hand, the hydration of DMPC results in water filling the highly polar interbilayer spaces with the resulting width increase [31,32]. This phenomenon might allow the incorporation of UA into DMPC bilayers and thus inducing the consequent structural perturbation (for further details regarding PC and PE fully hydrated gel phases, see ref. [33,34]).

DSC is a very sensitive method to investigate the alteration induced in the bilayer packing by guest substances. Generally, the pretransition of phosphatidylcholines is much more affected than the main phase transition and thus the first is considered as an indicator of the presence and level of foreign compounds in the lipid bilayer. In line with this reasoning, it was observed the distortion of pretransition for DMPC liposomes with 0.1 mM UA, and its disappearance at the content of 0.5 mM. Based on the DSC data, the pretransition has been associated with conformational rearrangement of the head group region of the lipid molecule [32,35,36]. On the other hand, fluorescence [37] and NMR [38,39] studies indicated that the pretransition had a significant effect on the arrangement of the acyl chains. Nadvorny and co-workers [40] characterized the interaction of UA with DPPC and DOPC by means of molecular dynamics simulations, and revealed that the UA molecules are distributed on the polar–nonpolar membrane interface. Moreover, the density profiles showed a correspondence in the distribution of UA and the phosphate groups of the lipids. Such location of the UA molecules corroborates well with our findings that in contrast to pretransition main phase transition of DMPC is altered only slightly in the presence of this compound. However, the lowering of T_m and by far an increase in peak width suggest that the chain melting is also affected by the presence of the UA molecules and consequently it can be hypothesized that they penetrate to some extent into this bilayer region. The assumption that UA molecules interact with the hydrocarbon lipid chains is in agreement with the X-ray results and those of Campanella and co-workers [41]; they applied spin–lattice relaxation 1H NMR techniques to establish the importance of apolar interactions (associated to the "hydrophobic forces") when UA molecules became entrapped in the interior of phospholipid bilayers. Worth noting is the fact that the distortion of DMPC main phase transition is not concentration-dependent. In the case of UA content higher than 0.5 mM, no further T_m shift and changes in the peak width were observed indicating the maximum incorporation, *i.e.*, bilayer saturation. In accordance with our findings, based on the calculated values of the free energy of mixing Andrade and co-workers noted that the DPPC/UA system had the best mixed character at low pressure and when the molar fraction of the UA was 0.5 [42]. Additionally, they proved a better interaction between UA and DOPC molecules due to the unsaturated nature of the lipid chain, which ensures a higher fluidity of the lipid matrix.

The thermal behavior of DMPE/UA liposomes considerably differs from that observed in the DMPC/UA ones since even at very low DMPE/UA ratio the transition peaks were significantly lowered and broaden. Additionally, DSC peak observed in the presence of UA at concentrations reaching 2 mM developed to a separate peak, which initially appeared at 49.68 °C, and was gradually shifted to 49.02 °C and 48.68 °C upon the consecutive heating scans. The two peaks in the DSC diagram indicate phase transition processes that can be attributed to two forms of DMPE/UA aggregates. Consequently, the 'solution-like' model, which agrees well with experimental data [43] for many lipophilic compounds fails for DMPE liposomes in the presence of UA molecules. In this model, it is assumed that during the melting, foreign substances are statistically distributed between the gel and liquid crystal phase and both the decrease in the phase transition temperature and the simultaneous increase in half width of the transition peak are linearly related to the concentration of guest molecules. On the contrary, it seems that DMPE/UA system could be described as a mixture of 'phase II' domains inserted within a structure of smaller and further ramified 'phase I' clusters consisting mainly of lipid molecules. This may be related to the ability of UA to form hydrogen bonds. Nadvorny [40] showed that the number of hydrogen bonds of UA with itself in its ionic form is higher compared to its neutral counterpart. Since it has been postulated that in physiological environment UA can assume its usniate form through a deprotonation at 3-OH, one can speculate that in the case of PE the increase in the number of UA–UA hydrogen bonds comes at the

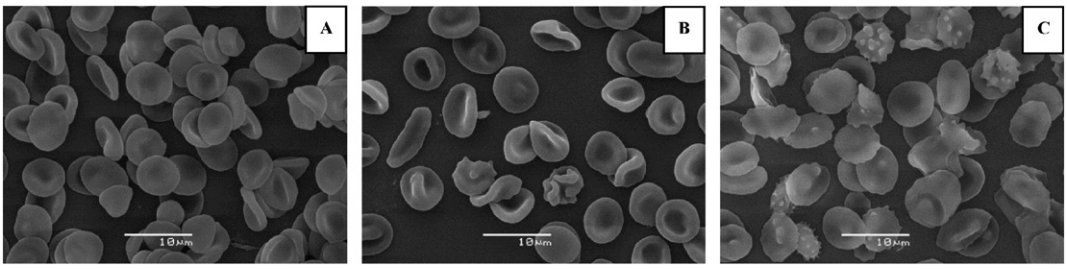

Fig. 7. Effects of usnic acid (UA) on the morphology of human erythrocytes. SEM images of (A) untreated erythrocytes; incubated with: (B) 10 μM UA, and (C) 1 mM UA.

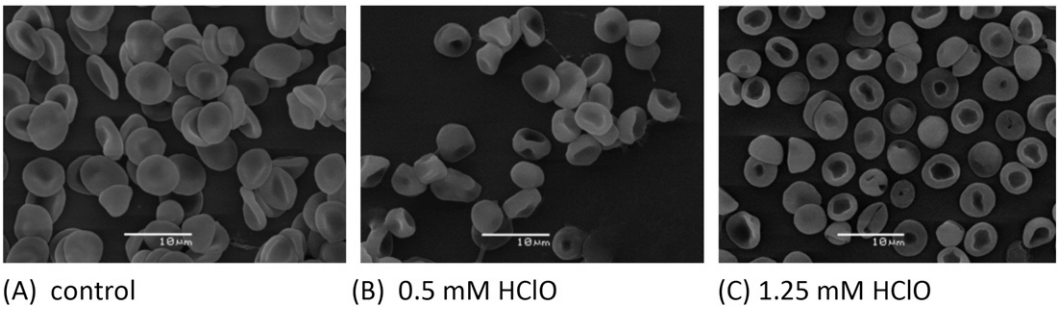

Fig. 8. Effect of HClO on the morphology of human erythrocytes. SEM images of (A) untreated erythrocytes; incubated with: (B) 0.5 mM HClO, and (C) 1.25 mM HClO.

expense of a decrease of the interaction between UA and the lipid phosphate groups resulting in the observed phase separation.

SEM and DM observations showed that UA induced morphological alterations to red cells from their normal discoid shape to echinocytes. These alterations were attained with usnic acid μM concentrations, lower than the mM concentrations used with DMPC and DMPE. This difference can be explained by the erythrocyte membrane higher fluidity. According to the bilayer couple hypothesis [44,45] shape changes induced in erythrocytes by foreign molecules are due to differential expansion of the two monolayers of the red cell membrane. Thus, stomatocytes are formed when the compound inserts into the inner monolayer whereas spiculate-shaped echinocytes are produced when it locates into the outer moiety. The finding that UA induced the formation of echinocytes, whose number increased with higher UA concentration, indicates that it was inserted in the outer leaflet of the erythrocyte membrane. It should be considered that an alteration of the normal biconcave shape of erythrocytes increases their resistance to entry into blood capillaries, which could contribute to a decreased blood flow, loss of oxygen, and tissue damage through microvascular occlusion [46,47]. Functions of ion channels, receptors and enzymes immersed in cell membrane lipid moieties also might be affected.

The antioxidant capacity of UA was assayed on DMPC and DMPE bilayers, as well as on human erythrocytes exposed to HClO-induced oxidative stress. HClO is an extremely toxic biological oxidant generated by neutrophils and monocytes, and it is considered one of the most important factors causing tissue injuries in inflammation [48]. It is directly toxic to bacteria, endothelial cells, tumor cells and red cells. However, because it readily reacts with a range of biological targets it has been difficult to identify which reactions are critical for its cytotoxic effects [49]. Human erythrocytes are a reliable and easily obtainable model to detect oxidative stress [50]. Their simple internal structure depleted of nucleus and organelles provides an ideal system for this type of study. One major consequence of their exposure to HClO is lysis; although the exact mechanism is not clear, the cell membrane is considered the primary site for reaction. In fact, several studies have demonstrated that HClO treatment of erythrocyte membrane results in inhibition of Na^+, K^+-, and Mg^{2+}-ATPase activities, oxidation of SH^- groups, tryptophan residues, chloramine formation, changes of membrane fluidity and

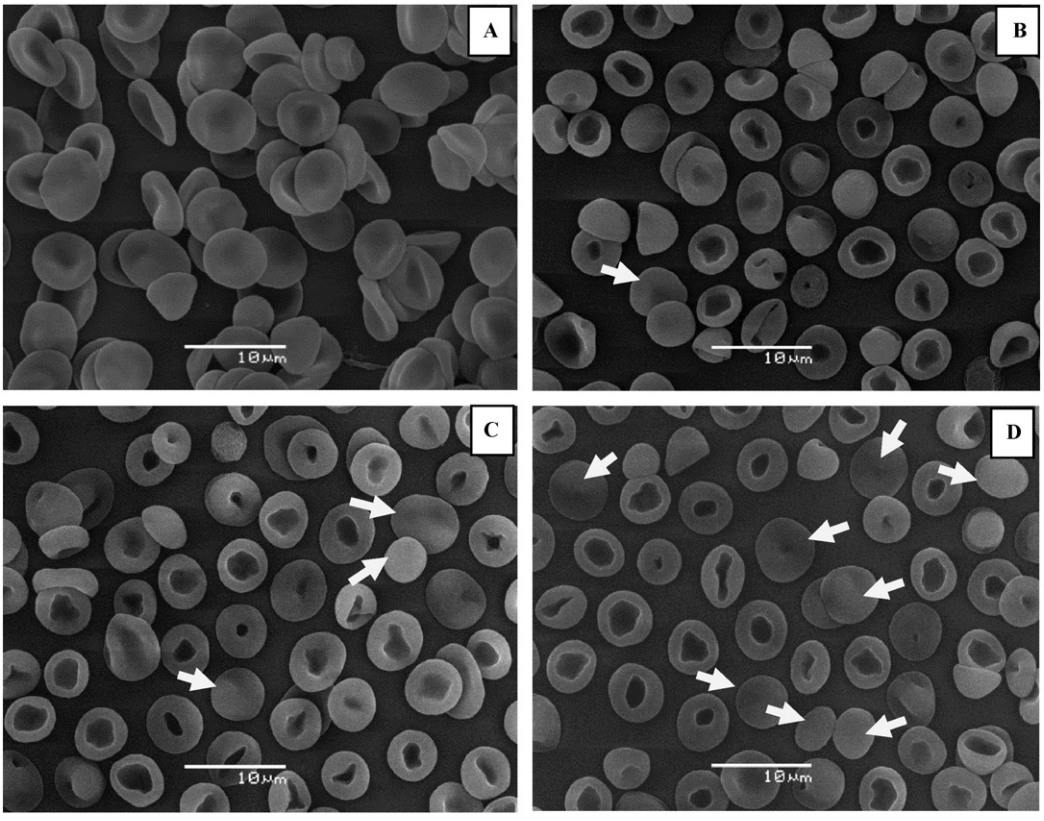

Fig. 9. Protective effects of usnic acid (UA) on the morphology of human erythrocytes. SEM images of (A) untreated erythrocytes; incubated with: (B) 1.25 mM HClO; (C) 2.5 μM UA and 1.25 mM HClO; (D) 7.5 μM UA and 1.25 mM HClO.

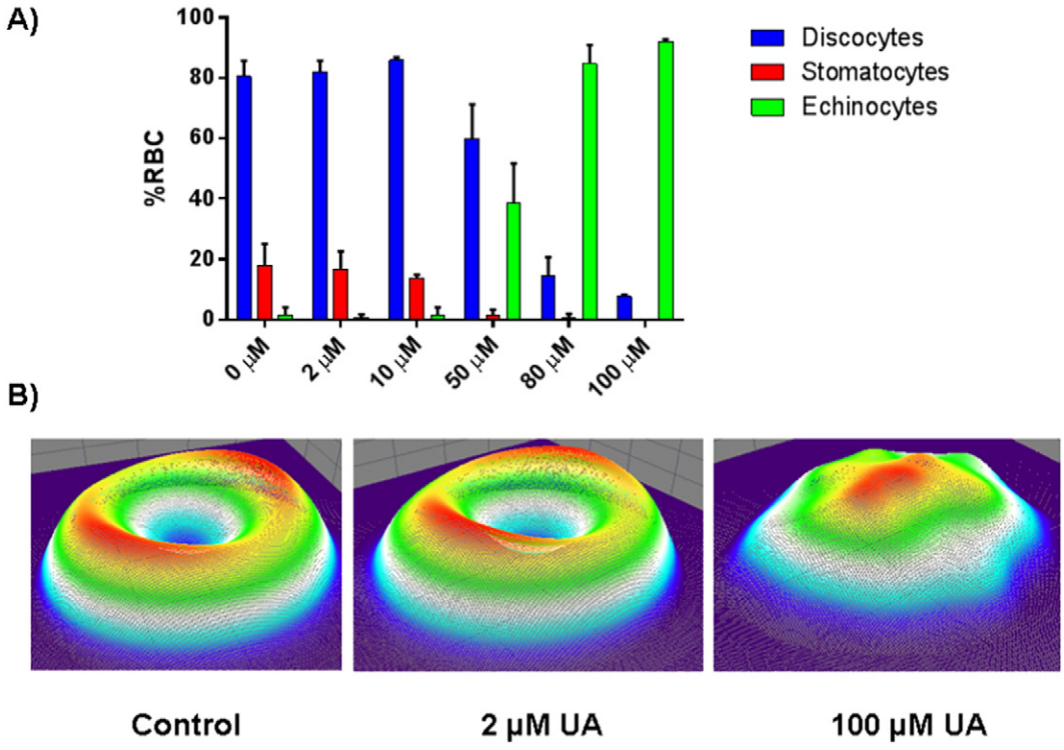

Fig. 10. DM observations of A) Population distribution of human erythrocytes with different concentrations of usnic acid (UA), and B) 3D reconstruction map of the thickness profile of red blood cells against 0 (control), 2 μM and 100 μM of usnic acid concentration.

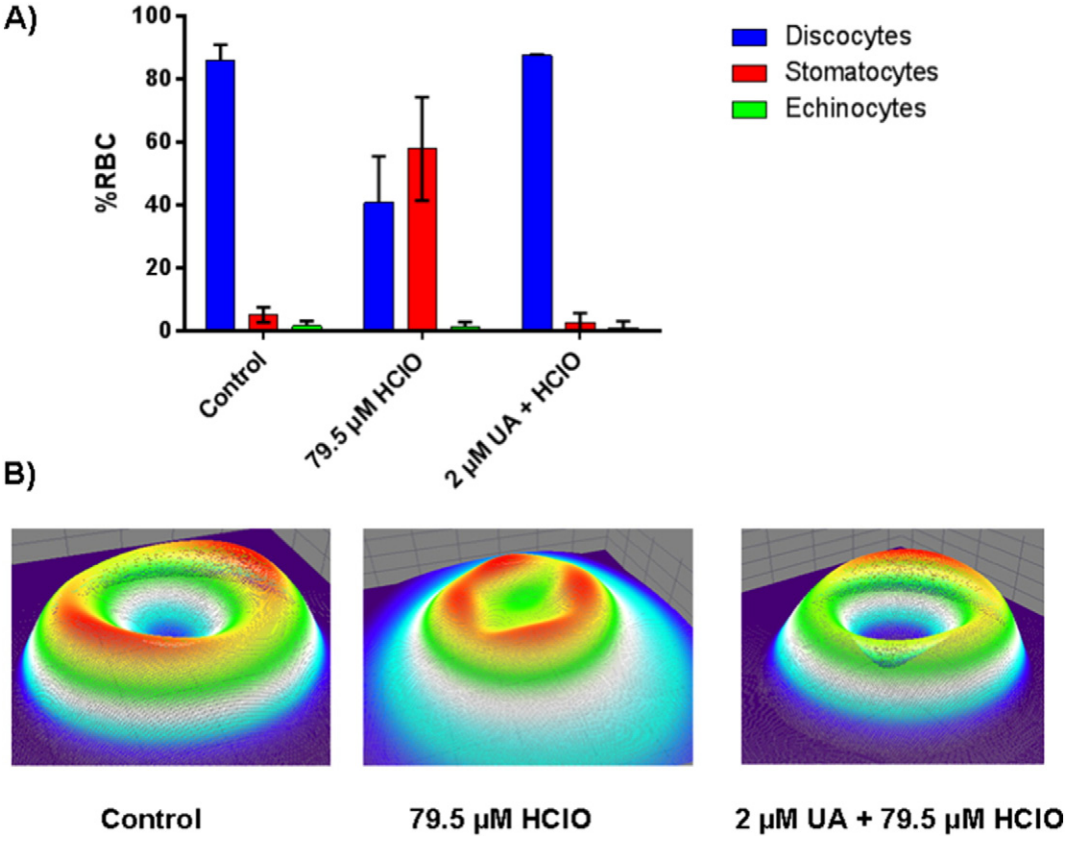

Fig. 11. DM observations of A) protective effect of usnic acid against human red blood cells exposed to HClO, and B) 3D reconstruction map of the thickness profile of the control RBC, at 79, 5 μM of HClO and with 79, 5 μM of HClO + 2 μM of usnic acid.

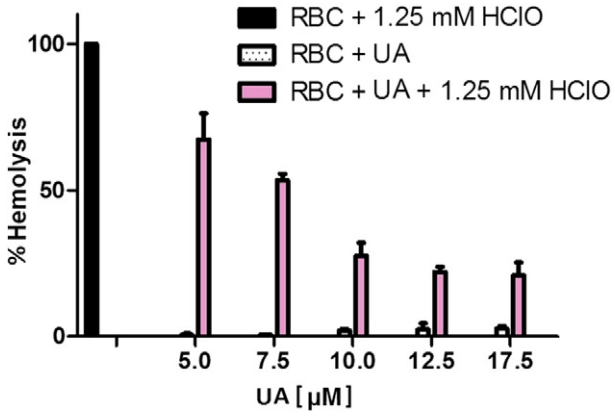

Fig. 12. Percentage of hemolysis of red blood cells (RBCs) incubated with 1.25 mM HClO and different concentrations of usnic acid (UA).

surface area, and membrane morphological transformations, events that precede cell lysis [48,49,51]. As shown in Fig. 3A and B, HClO perturbs to different extents the structures of DMPC and DMPE bilayers, being this effect higher in DMPE. Since both lipids possess the same fully saturated acyl chains of 14 methylene groups, the explanation for the dissimilar HClO effect must be related to the structural differences in their head group regions. In the case of DMPE, the adjacent molecules and bilayers are attached by a network of electrostatic interactions and H-bonds between the amino (H-donating) and phosphate (H-accepting) groups resulting in a very stable flat gel phase. HClO polar molecules (pK 7.53) would disrupt the H-bond net that keep together DMPE molecules by being intercalated between the negatively charged phosphates and positively charged amino groups. On the other hand DMPC head group, which instead of hydrogen is provided with a bulky methyl group, and with the presence of considerable amounts of water between the bilayers make the interbilayer interactions rather small. In this case, HClO molecules would remain mainly in the interbilayer water layers inducing perturbing effects at high concentrations by disruption of the intermolecular attractions in DMPC bilayer. In conclusion, UA molecules locate in the outer monolayer of the human erythrocyte membrane, interacting with the polar head groups and to some extent also with fatty acid chain region of the lipid bilayer. Thus, it would act as an antioxidant by blocking access of oxidants into cell membranes.

Conflict of interest

We do not have any conflict of interest.

Acknowledgments

To FONDECYT (research project 1130043 and postdoctoral project 3140167) and PIA-CONICYT PFB0824. DSC measurements were carried out with equipment purchased thanks to the financial support of the European Regional Development Fund within the framework of the Polish Innovation Economy Operational Program (contract No. POIG.02.01.00-12-167/08, project Malopolska Center of Biotechnology). Faculty of Biochemistry, Biophysics and Biotechnology of Jagiellonian University is a partner of the Leading National Research Center (KNOW) supported by the Ministry of Science and Higher Education.

References

[1] M. Cocchietto, N. Skert, P.L. Nimis, A review on usnic acid, an interesting natural compound, Naturwissenschaften 89 (2002) 137–146.
[2] P.A.S. White, R.C.M. Oliveira, A.P. Oliveira, M.R. Serafini, A.A.S. Araújo, D.P. Gelain, J.C.F. Moreira, J.R.G.S. Almeida, J.S.S. Quintans, L.J. Quintans-Juior, M.R.V. Santos, Antioxidant activity and mechanisms of action of natural compounds isolated from lichens: a systematic review, Molecules 19 (2014) 14496–14527.
[3] J.-q. Jin, Y. Rao, X.-l. Bian, A-g. Zeng, G.-d. Yang, Solubility of (+)-usnic acid in water, ethanol, acetone, ethyl acetate and *n*-hexane, J. Solut. Chem. 42 (2013) 1018–1027.
[4] K. Ingolfsdottir, Usnic acid, Phytochemistry 61 (2002) 729–736.
[5] L. Guo, Q. Shi, J.-L. Fang, N. Mei, A.A. Ali, S.M. Lewis, J.E.A. Leakey, V.H. Frankos, Review of usnic acid and *Usnea barbata* toxicity, J. Environ. Sci. Health C 26 (2008) 317–338.
[6] J.Y. Chen, W.H. Huestis, Role of membrane lipid distribution in chlorpromazine-induced shape change of human erythrocytes, Biochim. Biophys. Acta 1323 (1997) 299–309.
[7] J.M. Boon, B.D. Smith, Chemical control of phospholipid distribution across bilayer membranes, Med. Res. Rev. 22 (2000) 251–281.
[8] P.F. Devaux, A. Zachowsky, Maintenance and consequences of membrane phospholipids asymmetry, Chem. Phys. Lipids 73 (1994) 107–120.
[9] M. Suwalsky, P. Orellana, M. Avello, F. Villena, C.P. Sotomayor, Human erythrocytes are affected *in vitro* by extracts of *Ugni molinae* leaves, Food Chem. Toxicol. 44 (2006) 1393–1398.
[10] M. Suwalsky, P. Vargas, M. Avello, F. Villena, C.P. Sotomayor, Human erythrocytes are affected *in vitro* by *Aristotelia chilensis* (Maqui) leaves, Int. J. Pharm. 363 (2008) 85–90.
[11] M. Suwalsky, K. Oyarce, M. Avello, F. Villena, C.P. Sotomayor, Human erythrocytes and molecular models of cell membranes are affected *in vitro* by *Balbisia peduncularis* (Amancay) extracts, Chem. Biol. Interact. 179 (2009) 413–418.
[12] M. Manrique-Moreno, J. Londoño-Londoño, M. Jemiola-Rzeminska, K. Strzalka, F. Villena, M. Avello, M. Suwalsky, Structural effects of the *Solanum* steroids solasodine, diosgenin and solanine on human erythrocytes and molecular models of eukaryotic membranes, Biochim. Biophys. Acta 1838 (2014) 266–277.
[13] T. Tatsumi, H. Fliss, Hypochlorous acid and chloramines increase endothelial permeability: possible involvement of cellular zinc, Am. J. Physiol. 267 (1994) 1597–1607.
[14] L.B. Zavodnik, I.B. Zavodnik, E.A. Lapshyna, V.U. Buko, M.J. Bryszewska, Hypochlorous acid-induced membrane pore formation in red blood cells, Bioelectrochem. 58 (2002) 157–161.
[15] C.L. Hawkins, M.J. Davies, Hypochlorite-induced damage to proteins: formation of nitrogen-centred radicals from lysine residues and their role in protein fragmentation, J. Biochem. 332 (1998) 617–625.
[16] A.C. Carr, M.C.M. Vissers, N.M. Domigan, C.C. Witerbourn, Modification of red cell membrane lipids by hypochlorous acid and hemolysis by preformed lipid clorohydrins, Redox Rep. 3 (1997) 263–271.
[17] J.C. Morris, The acid ionisation of HOCl from 5 degree to 35 degree, J. Phys. Chem. 70 (1966) 3798–3805.
[18] B. Zimmermann, D.M. Soumpasis, Effects of monovalent cations on red cell shape and size, Cell Biophys. 7 (1985) 115–127.
[19] S.V.P. Malheiros, M.A. Brito, D. Brites, M.N. Correa, Membrane effects of trifluoperazine, dibucaine and praziquantel on human erythrocytes, Chem. Biol. Interact. 126 (2000) 79–95.
[20] S. Etcheverry, M. Gallardo, P. Solano, M. Suwalsky, O.N. Mesquita, C.J. Saavedra, Real-time study of shape and thermal fluctuations in the echinocyte transformation of human erythrocytes using defocusing microscopy, Biomed. Opt. 17 (2012) 1060131–1060136.
[21] L.G. Mesquita, U. Agero, O.N. Mesquita, Defocusing microscopy: an approach for red blood cell optics, Appl. Phys. Lett. 88 (2006) 133901–133903.
[22] P.M.S. Roma, L. Siman, F.T. Amaral, U. Agero, O.N. Mesquita, Total three-dimensional imaging of phase objects using defocusing microscopy: application to red blood cells, Appl. Phys. Lett. 104 (2014) 251107.
[23] M.A. Vives, M.R. Infante, E. Garcia, C. Selve, M. Maugras, M.P. Vinardell, Erythrocyte hemolysis and shape changes induced by new lysine-derivate surfactants, Chem. Biol. Interact. 118 (1999) 1–18.
[24] E. Beutler, Red Cell Metabolism. A manual of Biochemical Methods, Grune & Straton, New York, 1975.
[25] M. Suwalsky, Phospholipid bilayers, in: J.C. Salamone (Ed.)Polymeric Materials Encyclopedia, vol. 7, CRC, Boca Raton, FL 1996, pp. 5073–5078.
[26] D. Marsh, General features of phospholipid phase transitions, Chem. Phys. Lipids 57 (1991) 109–120.
[27] R. Koynova, M. Caffrey, Phases and phase transitions of the phosphatidylcholines, Biochim. Biophys. Acta 1376 (1998) 91–145.
[28] R.N. Lewis, R.N. McElhaney, Calorimetric and spectroscopic studies of the polymorphic phase behavior of a homologous series of n-saturated 1,2-diacyl phosphatidylethanolamines, Biophys. J. 64 (1993) 1081–1096.
[29] R.S. Foti, L.J. Dickmann, J.A. Davis, R.J. Geene, J.J. Hill, M.L. Howard, J.T. Pearson, D.A. Rock, J.C. Tay, J.L. Wahlstrom, J.G. Slatter, Metabolism and related human risk factors for hepatic damage by usnic acid containing nutritional supplements, Xenobiotica 38 (2008) 264–280.
[30] A. Lamprecht, J.L. Saumet, J. Roux, J.P. Benoit, Lipid nanocarriers as drug delivery system for ibuprofen in pain treatment, Int. J. Pharm. 278 (2004) 407–411.
[31] M. Suwalsky, L. Duk, X-ray studies on phospholipid bilayers, 7. Structure determination of oriented films of L-α-dimyristoylphosphatidylethanolamine (DMPE), Makromol. Chem. 188 (1987) 599–606.
[32] M.J. Janiak, D.M. Small, G.G. Shipley, Nature of the thermal pretransition of synthetic phospholipids: dimyristoyl- and dipalmitoyllecithin, Biochemistry 15 (1976) 4575–4580.
[33] J. Katsaras, S. Tristram-Nagle, Y. Liu, R.L. Headrick, E. Fontes, P.C. Mason, J. Nagle, Clarification of the ripple phase of lecithin bilayers using fully hydrated, aligned samples, Phys. Rev. E 61 (2000) 5668–5677.

[34] P.C. Mason, J.F. Nagle, R.M. Epand, J. Katsaras, Anomalous swelling in phospholipid bilayers is not coupled to the formation of a ripple phase, Phys. Rev. E 63 (2001) 309021–309024.
[35] D. Chapman, Fluidity and phase transition of cell membranes, in: H. Eisenberg, E. Katchalsky-Katzir, L.A. Manson (Eds.), Biomembranes, vol. 7, Springer, N.Y., USA 1975, pp. 1–9.
[36] M.J. Janiak, D.M. Small, G.G. Shipley, Temperature and compositional dependence of the structure of hydrated dimyristoyl lecithin, J. Biol. Chem. 254 (1979) 6068–6072.
[37] K. Jacobson, D. Papahadjopoulos, Phase transitions and phase separations in phospholipid membranes induced by changes in temperature, pH, and concentration of bivalent cations, Biochemistry 14 (1975) 152–156.
[38] T.J. Mclntosh, Difference in hydrocarbon chain tilt between hydrated phosphatidylethanolamine and phosphatidylcholine bilayers: a molecular packing model, Biophys. J. 29 (1980) 237–241.
[39] E. Boroske, L. Trahms, A 1H and 13C NMR study of motional changes of dipalmitoyl lecithin associated with the pretransition, Biophys. J. 42 (1983) 275–281.
[40] D. Nadvorny, J.B. da Silva, R.D. Lins, Anionic form of usnic acid promotes lamellar to nonlamellar transition in DPPC and DOPC membranes, J. Phys. Chem. B 118 (2014) 3881–3886.
[41] L. Campanella, M. Delfini, P. Ercole, A. Iacoangeli, G. Risuleo, Molecular characterization and action of usnic acid: a drug that inhibits proliferation of mouse polyomavirus in vitro and whose main target is RNA transcription, Biochimie 84 (2002) 329–334.
[42] C.A.S. Andrade, N.S. Santos-Magalhaes, C.P.D., Melo, Thermodynamic characterization of the prevailing molecular interactions in mixed floating monolayers of phospholipids and usnic acid, J. Colloid Interface Sci. 298 (2006) 145–153.
[43] A.G. Lee, Lipid phase transitions and phase diagrams. II. Mixtures involving lipids, Biochim. Biophys. Acta 472 (1977) 285–344.
[44] M.P. Sheetz, S.J. Singer, Biological membranes as bilayer couples. A molecular mechanism of drug–erythrocyte induced interactions, Proc. Natl. Acad. Sci. U. S. A. 71 (1974) 4457–4461.
[45] G. Lim, M. Wortis, R. Mukhopadhyay, Stomatocyte–discocyte–echinocyte sequence of the human red blood cell: evidence for the bilayer-couple hypothesis from membrane mechanics, Proc. Natl. Acad. Sci. 99 (2002) 16766–16769.
[46] S.L. Winski, D.E. Carter, Arsenate toxicity in human erythrocytes: characterization of morphological changes and determination of the mechanism of damage, J. Toxicol. Environ. Health A 53 (1998) 345–355.
[47] S. Svetina, D. Kuzman, R.E. Waugh, P. Zibert, B. Zeks, The cooperative role of membrane skeleton and bilayer in the mechanical behaviour of red blood cells, Bioelectrochemistry 62 (2004) 107–113.
[48] I.B. Zavodnik, E.A. Lapshina, L.B. Zavodnik, G. Bartosz, M. Soszynski, M. Bryszewska, Hypochlorous acid damages erythrocyte membrane proteins and alters lipid bilayer structure and fluidity, Free Radic. Biol. Med. 30 (2001) 363–369.
[49] M.C.M. Vissers, A.C. Carr, A.L.P. Chapman, Comparison of human red cell lysis by hypochlorous and hypobromous acids: insights into the mechanism of lysis, Biochem. J. 330 (1998) 131–138.
[50] M. Battistelli, R. De Sanctis, R. De Bellis, L. Cucchiarini, M. Dachà, P. Gobbi, *Rhodiola rosea* as antioxidant in red blood cells: ultrastructural and hemolytical behavior, Eur. J. Histochem. 49 (2005) 243–254.
[51] M.C.M. Vissers, C.C. Winterbourn, Oxidation of intracellular glutathione after exposure of human red blood cells to hypochlorous acid, Biochem. J. 307 (1995) 57–62.